Journal of Luminescence 129 (2009) 1304–1308

Contents lists available at ScienceDirect

Journal of Luminescence

journal homepage: www.elsevier.com/locate/jlumin

A series of Eu(III) emitters with a novel triphenylamine-derived beta-diketone ligand

Liming Zhang [a,b], Bin Li [a,*]

[a] Key Laboratory of Excited State Processes, Changchun Institute of Optics Fine Mechanics and Physics, Chinese Academy of Sciences, Changchun 130033, PR China
[b] Graduate School of the Chinese Academy of Sciences, Chinese Academy of Sciences, Beijing 100039, PR China

ARTICLE INFO

Article history:
Received 15 December 2008
Received in revised form
13 June 2009
Accepted 18 June 2009
Available online 24 June 2009

Keywords:
Europium complexes
Photoluminescence
Excited state lifetime
Triphenylamine

ABSTRACT

In this paper, a series of Eu(III)complexes with a novel triphenylamine-derived beta-diketone ligand are synthesized. Systematical research reveals that these Eu(III) complexes take an occasional antenna mechanism by transferring energy between singlet state of ligand and central Eu(III), which leads to much shortened excited state lifetimes of the corresponding Eu(III) complexes.

1. Introduction

Organic light-emitting diodes (OLEDs) have been intensively studied throughout the world owing to their potential applications in the next generation of full-color flat panel displays [1–3]. For commercial applications, three primary colors of blue, green and red are basically required. Organolanthanide complexes are a species of important organic electroluminescence (EL) materials. Owing to the unique f-electron configurations, lanthanide-based emitter can not only generate extremely pure emission, but also offer an unlimited theoretical ceiling for device efficiency. Furthermore, the physical properties pertinent to processability of these materials can be conveniently altered without affecting the metal-based emission characteristics [4].

Kido et al. first reported an EL device using $Eu(TTA)_3 \cdot 2H_2O$ (TTA = 2-thenoyltrifluoroacetonate) as the emitter, which sparked the utilization of organoeuropium complexes in the field of red-emitting OLEDs [5]. Up to now, one of the best Eu-complex-based EL devices is realized by Huang et al. with the maximum brightness of $2000\,cd/m^2$ at 20 V and the maximum power efficiency of 2.7 lm/W [6]. Although have been improved largely, these parameters are still unsatisfactory when compared with those of EL devices based on pure organic emitters and phosphorescent emitters. Li et al. found in their lanthanide-based OLEDs that, after reaching the maximum value, the efficiency decreases as the current density increases in the high current density region. It is proposed that the excited state quenching of Eu-complex caused by charge carrier should be partly responsible for the efficiency decrease [7]. Similarly, Forrest, Thompson and Adachi pointed out that, for most of phosphorescent OLEDs as well as lanthanide-emitter-based OLEDs, the device quantum efficiencies drop rapidly with increasing current density [8]. Detailed research suggests that this quantum decrease is caused by the long excited state lifetime. In addition, two possible triplet exciton quenching mechanisms, triplet–triplet (T–T) annihilation and polaron–triplet (P–T) annihilation, have been proposed. It is claimed that T–T annihilation exerts a significant effect on all systems where triplet excitons possess $\sim 1\,\mu s$ lifetimes and participate in energy transfer (ET). And the quantum efficiency roll-off is arguably the most significant problem facing lanthanide-emitter-based OLEDs.

Aiming at actualizing high efficiency and sharp red emission from europium-based emitter, it is necessary to explore short-lived organoeuropium emitters. In this paper, a new triphenylamine-derived ligand and its corresponding Eu(III) complexes are synthesized to explore the strongly needed red-emitting short-lived emitters.

2. Experimental section

Molecular structures of ligands and complexes are shown in Scheme 1.

1,3-diphenyl-propane-1,3-dione (DBM), 1,10-phenanthroline (Phen), 4,5,9,13,14,18-hexaaza-phenanthro-9,10-triphenylene (TPPHZ),

---

[*] Corresponding author. Tel./fax: +86 431 86176935.
E-mail address: lib020@yahoo.cn (B. Li).

0022-2313/$ - see front matter © 2009 Elsevier B.V. All rights reserved.
doi:10.1016/j.jlumin.2009.06.015

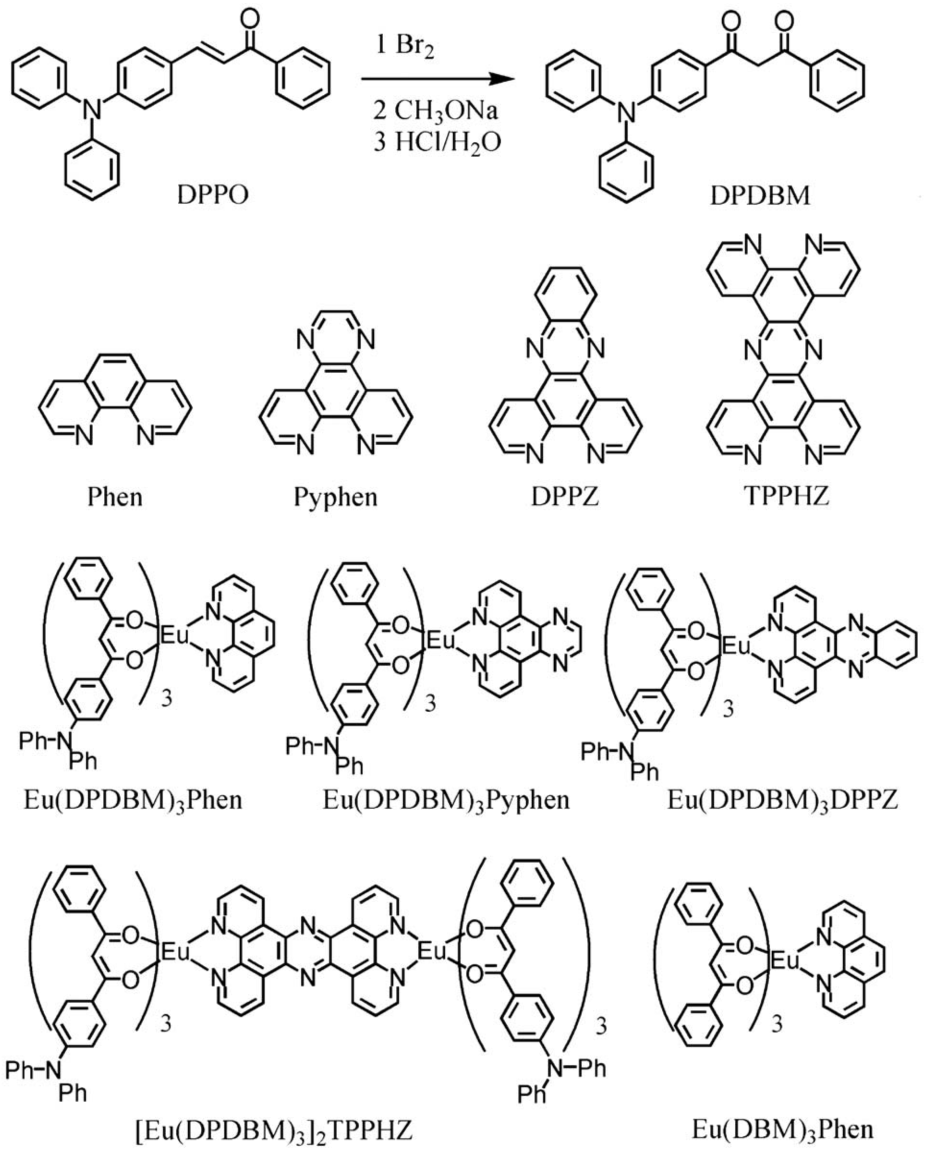

Scheme 1. Molecular structures of ligands and complexes.

ethane-1,2-diamine and benzene-1,2-diamine were purchased from Aldrich Chemical Co. and used without further purification.

The synthetic route of 1-(4-diphenylamino-phenyl)-3-phenyl-propane-1,3-dione (DPDBM) is shown in Scheme 1: the starting material 3-(4-diphenylamino-phenyl)-1-phenyl-propenone (DPPO) was synthesized according to our previous report [9]. The mixture of 3 mL of Br_2, 10 mmol of DPPO, and 10 mL of CCl_4 was stirred at 0 °C for 30 min. The resulting solid was washed with hot EtOH, and then added into the solution of 2.3 g of Na and 23 mL of MeOH. The mixture was refluxed for 1 h at 80 °C. After cooling, the solution was neutralized with 10 mL of HCl, and then refluxed for 30 min at 100 °C. The crude product was collected at 0 °C and further purified by recrystalization in a mixed solvent of MeOH/EtOH [10]. ^{1}H NMR ($CDCl_3$): δ 8.22 (s, 1H), 7.99-7.97 (m, 2H), 7.93 (s, 1H), 7.87-7.84 (m, 2H), 7.79-7.58 (m, 4H), 7.50-7.35 (m, 5H), 7.10 (s, 1H), 6.97 (s, 1H), 6.67 (s, 1H) 6.52 (s, 1H), 3.26 (s, 1H). Anal. Calcd. For $C_{27}H_{21}NO$: C, 86.37; H, 5.64; N, 3.73. Found: C, 86.21; H, 5.71; N, 3.56.

[1,10] phenanthroline-5,6-dione was synthesized exactly according to the literature procedure [11].

A typical synthetic procedure for 1,4,8,9-tetraaza-triphenylene (Pyphen) and 4,5,9,14-tetraaza-benzotriphenylene (DPPZ) is described as follows: the mixture of 5 mmol of 1,10-phenanthroline-5,6-dione, 5.5 mmol of diamine, 25 ml of ethanol and 0.05 mmol of 4-methylbenzenesulfonic acid was heated under 80 °C for 10 h, the crude product was filtered and then recrystallized from ethanol to give the pure desired product.

Pyphen: colorless crystal. ^{1}H NMR ($CDCl_3$): δ 9.51(d, 2 H, $J = 8.0$ Hz), 9.31(d, 2 H, $J = 8.0$ Hz), 9.01(s, 2 H), 7.82(dd, 2 H, $J = 8.0$, 8.0 Hz). Anal. Calcd. For $C_{14}H_8N_4$: C, 72.41; H, 3.45; N, 24.14. Found: C, 72.24; H, 3.48; N, 23.98.

DPPZ: light brown crystal. ^{1}H NMR ($CDCl_3$): δ 9.65(d, 2H, $J = 8.0$ Hz), 9.27(d, 2H, $J = 8.0$ Hz), 8.35(d, 2H, $J = 6.4$ Hz), 7.91(d, 2H, $J = 6.4$ Hz), 7.80(dd, 2H, $J = 8.0$, 8.0 Hz). Anal. Calcd. For $C_{18}H_{10}N_4$: C, 76.60; H, 3.55; N, 19.86. Found: C, 75.95; H, 3.61; N, 19.81.

Eu(III) complexes were synthesized according to the literature procedure [12].

Eu(DPDBM)$_3$Phen. Anal. Calcd. For $C_{93}H_{68}N_5O_6Eu$: C, 74.29; H, 4.56; N, 4.66. Found: C, 74.37; H, 4.33; N, 4.57.

Eu(DPDBM)$_3$Pyphen. Anal. Calcd. For $C_{95}H_{68}N_7O_6Eu$: C, 73.35; H, 4.41; N, 6.30. Found: C, 73.21; H, 4.50; N, 6.37.

Eu(DPDBM)$_3$DPPZ. Anal. Calcd. For $C_{99}H_{70}N_7O_6Eu$: C, 74.06; H, 4.39; N, 6.11. Found: C, 74.13; H, 4.28; N, 6.18.

[Eu(DPDBM)$_3$]$_2$TPPHZ. Anal. Calcd. For $C_{186}H_{132}N_{12}O_{12}Eu_2$: C, 73.70; H, 4.39; N, 5.55. Found: C, 73.78; H, 4.47; N, 5.43.

Eu(DBM)$_3$Phen. Anal. Calcd. For $C_{57}H_{41}N_2O_6Eu$: C, 68.33; H, 4.12; N, 2.80. Found: C, 68.21; H, 4.30; N, 2.96.

Luminescent lifetimes were obtained with a 355 nm light generated from the third-harmonic-generator pumped, which using pulsed Nd:YAG laser as excitation source. The Nd:YAG laser possesses a line width of 1.0 cm^{-1}, pulse duration of 10 ns and repetition frequency of 10 Hz. A Rhodamine 6 G dye pumped by the same Nd:YAG laser was used as the frequency-selective excitation source. All the photoluminescence (PL) spectra were measured with a Hitachi F-4500 fluorescence spectrophotometer. Triplet state energy of DPDBM was measured at low temperature (77 K). UV–vis absorption spectra were recorded using a Shimadzu UV-3101PC spectrophotometer. ^{1}H spectra were obtained with the use of a Varian INOVA 300 spectrometer. Elemental analyses were performed on a Carlo Erba 1106 elemental analyzer. Photoluminescence quantum efficiencies were measured using a literature procedure [9]. All measurements were carried out in the air at room temperature without being specified.

3. Results and discussion

3.1. UV–vis absorption and photoluminescence

3.1.1. UV–vis absorption and excitation spectra

Fig. 1 shows the absorption spectra of Eu(DPDBM)$_3$Phen, Eu(DPDBM)$_3$Pyphen, Eu(DPDBM)$_3$DPPZ and [Eu(DPDBM)$_3$]$_2$TPPHZ as well as that of beta-diketone ligand, DPDBM. Obviously, the absorption spectra of DPDBM-based Eu(III) complexes demonstrate DPDBM's absorption character by peaking at 378, 298 and 230 nm, respectively, suggesting that their absorption are mainly composed of DPDBM's electronic transition. The strengthened absorption bands centering at ~250 nm are assigned as absorption of diimine ligands as previously reported [13]. Compared with excitation spectra of Eu(DPDBM)$_3$Phen, Eu(DPDBM)$_3$Pyphen, Eu(DPDBM)$_3$DPPZ and [Eu(DPDBM)$_3$]$_2$TPPHZ shown in Fig. 2, their excitation maxima (~412 nm) are, thus, assigned as photo absorption/excitation of DPDBM. Excitation spectral blue shift of the Eu(III) complexes compared with that of free DPDBM as shown in Fig. 2 can be easily explained by coordination effect which causes electron density decrease of DPDBM. While, spectral red shifts are found from comparison between excitation and absorption spectra of the Eu(III) complexes, which can be explained as follows. As we reported, in triphenylamine-derived compounds, the onset electronic transition type is an $n \rightarrow \pi^*$ one whose molar extinction coefficient is much smaller than that of the following higher energy $\pi \rightarrow \pi^*$ transition [9]. Consequently, higher energy $\pi \rightarrow \pi^*$ transition covers up the $n \rightarrow \pi^*$ transition, leading to a spectral shift towards shorter wavelength.

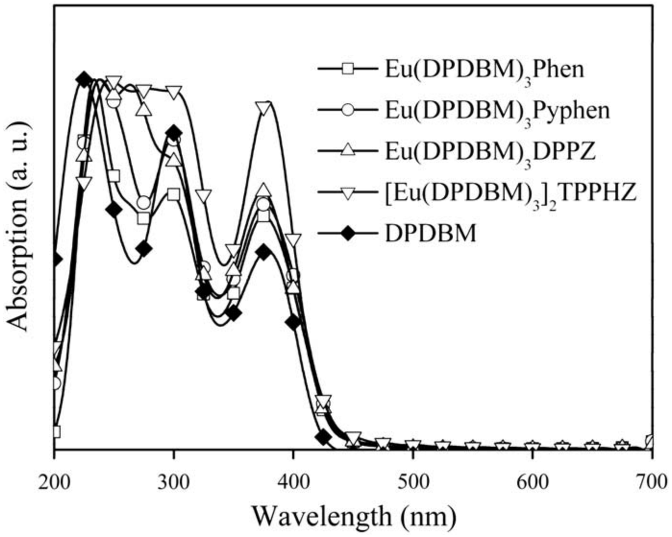

Fig. 1. Absorption spectra of the Eu(III) complexes and DPDBM in CH_2Cl_2 with a concentration of 1×10^{-5} mol/L.

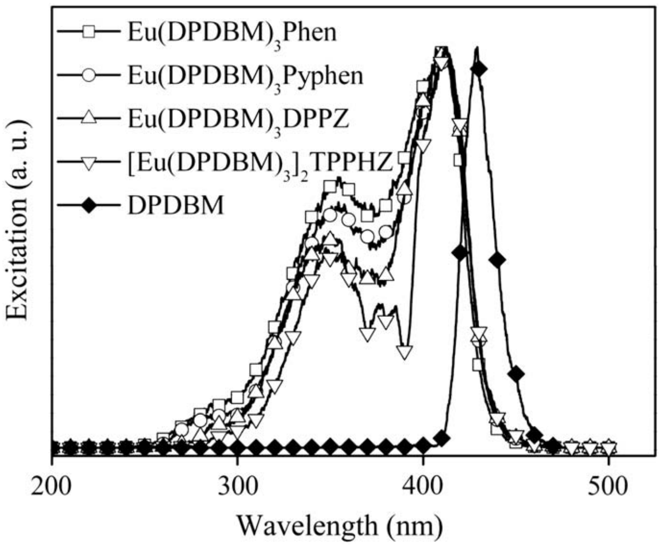

Fig. 2. Excitation spectra of the Eu(III) complexes ($\lambda_{em} = 612$ nm) and DPDBM ($\lambda_{em} = 475$ nm) in CH_2Cl_2 with a concentration of 1×10^{-5} mol/L.

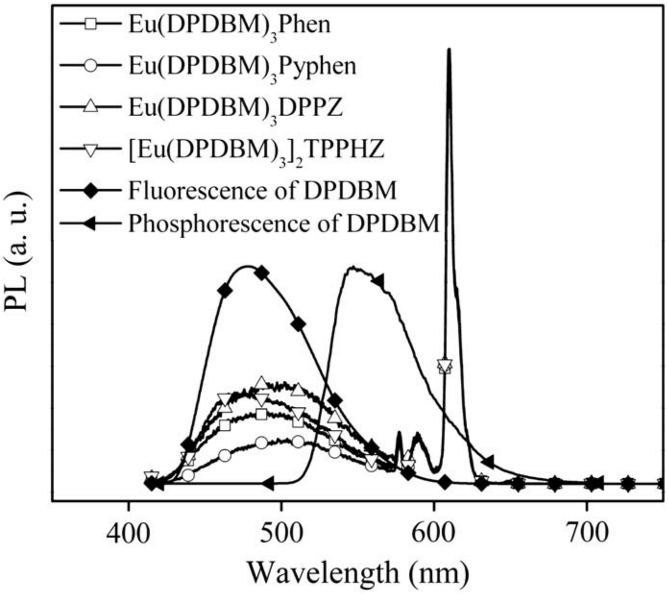

Fig. 3. PL spectra of Eu(III) complexes and DPDBM in CH_2Cl_2 with a concentration of 1×10^{-5} mol/L as well as phosphorescence of DPDBM at 77 K.

3.1.2. PL spectra

The PL spectra of Eu(DPDBM)$_3$Phen, Eu(DPDBM)$_3$Pyphen, Eu(DPDBM)$_3$DPPZ and [Eu(DPDBM)$_3$]$_2$TPPHZ shown in Fig. 3

Table 1
Emission peaks and PL efficiencies of the Eu(III) complexes.

Complex	Emission peaks (nm)[a]	Total efficiency[b]	Eu^{3+} contribution[b]
$Eu(DPDBM)_3Phen$	493, 610	0.79	0.30
$Eu(DPDBM)_3Pyphen$	505, 609	0.48	0.24
$Eu(DPDBM)_3DPPZ$	497, 610	0.56	0.17
$[Eu(DPDBM)_3]_2TPPHZ$	468, 608	0.71	0.24

[a] ±1 nm.
[b] ±5%.

suggest that there are two emissive centers in each complex: one is DPDBM, showing an emission peaking at ~500 nm; the other is Eu(III) ion, giving the character emission band peaking at 610 nm. The total PL quantum efficiencies as well as Eu(III)'s contributions to total efficiencies are measured and summarized in Table 1. Although energy transfer between DPDBM and Eu(III) ion seems to be somewhat incomplete because of DPDBM's singlet emission, PL efficiency fractions of Eu(III) ion are still remarkable. According to the previous report, there are three mechanisms for intramolecular energy transfer in organolanthanide complexes [14]. Mechanism A: after an efficient intersystem crossing between the lowest singlet and triplet excited states of the ligand, energy transfer from T_1 to a lower energy state of the lanthanide(III) ion. Mechanism B: there is a direct energy transfer from S_1 to a lower energy state of the lanthanide(III) ion. Mechanism C: there is an energy transfer from S_1 to an upper intermedia level of the lanthanide(III) ion, then back to T_1 to return finally to a lower energy level of the lanthanide(III) ion before emitting. It is claimed that mechanism A seems to agree with most of the experimental results obtained by various research groups. However, in this report, we suggest that mechanism B should be the major ET mechanism. A schematic representation of the energy transfer process is given in Fig. 4. We are giving an explanation as follows. The energy transfer factor, F_{ET}, is expressed by Formula (1), where Φ_L and Φ_{RE} stand for the excited state energy levels of ligand and lanthanide(III) ion, respectively [15].

$$F_{ET} = \int \Phi_L(E)\Phi_{RE}(E)dE \tag{1}$$

Formula (1) suggests that there is an optimal energy difference region within which the most efficient energy transfer from Φ_L to Φ_{RE} occurs. As for Eu(III), the optimal value localizes between 2000 and 5000 cm^{-1}. As shown in Fig. 3, the singlet state and triplet state of DPDMB are measured to be 20,920 and 18,340 cm^{-1}, respectively. The singlet state energy localizes within the optimal region, while the triplet state energy of DPDBM is obviously too small for efficient energy transfer to central ion (17500 cm^{-1}). In addition, DPDBM's singlet emission is found in all PL spectra of the Eu(III) complexes, suggesting that triplet excited state formation of DPDBM is largely suppressed by its singlet state radiative decay process. Thus, it is concluded that, in these Eu(III) complexes, dominating ET process happens between DPDBM's singlet state and Eu(III) ion.

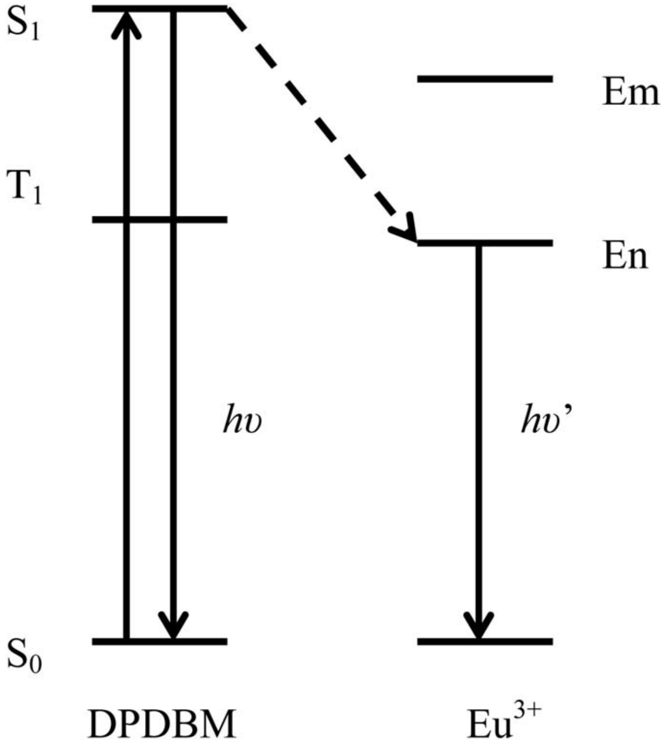

Fig. 4. Energy transfer process between ligand and central ion.

Table 2
Measured excited state lifetimes ($\lambda = 610$ nm) and calculated Judd–Ofelt parameters.

Complex	τ (μs)[a]	A_{MD} (S^{-1})	Ω_2 (cm^2)	$A_{^5D_0\rightarrow ^7F_2}$ (S^{-1})
$Eu(DPDBM)_3Phen$	40	34.7	7.06	185
$Eu(DPDBM)_3Pyphen$	40	34.6	7.48	196
$Eu(DPDBM)_3DPPZ$	20	34.9	6.38	167
$[Eu(DPDBM)_3]_2TPPHZ$	40	34.6	7.50	196
$Eu(DBM)_3Phen$	140	34.9	12.97	340

[a] ±5%.

3.2. Excited state lifetimes

As we mentioned, emitters with short excited state lifetimes are strongly needed to over come efficiency roll-off in OLEDs. The experimentally recorded $^5D_0 \rightarrow {}^7F_2$ radiative lifetimes (τ) are summarized in Table 2. It is worth notable that they are typically one order of magnitude smaller than the previously reported ones. Thus, the radiative/inradiative decay process should be further discussed to explore the correlation between ligand coordination sphere and excited state lifetime. However, considering that there are two emissive centers in each of the Eu(III) complexes, which means two pairs of radiative and inradiative decay processes, the general quantum efficiency expression given as Formula (2) is, thus, invalid to depict specific radiative/inradiative decay details of each process.

$$\Phi = \frac{K_r}{K_r + K_{nr}} \tag{2}$$

The Judd–Ofelt theory has been successful in understanding and predicting the spectral intensities of the induced electric dipole (ED) transitions. According to Judd–Ofelt theory, the magnetic dipole (MD) and induced electric dipole spontaneous emission probability, A_{MD} and A_{ED}, are given by Formula (3) and (4), where (2J+1) is the multiplicity of the upper state, n the refractive index, e the electron charge and υ the emission peak (in wave number).

$$A_{MD} = \left[\frac{64\pi^4 \nu^3}{3h(2J+1)}\right] n^3 S_{MD} \tag{3}$$

$$A_{\mathrm{ED}}=\left[\frac{64\pi^4 e^2 \nu^3}{3h(2J+1)}\right]\frac{n(n^2+2)^2}{9}\sum_{t=2,4,6}\Omega_t|\langle f^N\Psi_J\|U^{(t)}\|f^N\Psi'_{J'}\rangle|^2 \qquad (4)$$

The three phenomenological Judd–Ofelt parameters, Ω_2, which is related to the short-range effects such as coordination sphere, covalency and structural changes in the vicinity of Eu(III), Ω_4, which is related to the long-range effects, and Ω_6, can be calculated from emission spectra and using the matrix elements of Weber and Carnall [16]. The radiative transitions within the [Xe]$4f^6$ configuration of Eu(III) are parity forbidden and consist mainly of weak magnetic dipole and induced electric dipole transitions. The probabilities of MD transitions are independent of the chemical environment of the ion, in contrast to those of the ED transitions. The $^5D_0\rightarrow{}^7F_{0,3}$ transitions at ~579 and ~650 nm, respectively, are very weak as shown in Fig. 3. A more detailed analysis has indicated that these transitions borrow intensity from the strong $^5D_0\rightarrow{}^7F_2$ transition through higher order perturbations by the ligand field and cannot be accounted for by either the MD mechanism or the Judd–Ofelt theory. The $^5D_0\rightarrow{}^7F_1$ emission around 593 nm, however, is a pure MD transition. The strongest emission is observed around 610 nm corresponding to the $^5D_0\rightarrow{}^7F_2$ transition. The spectra all show splitting of the $^5D_0\rightarrow{}^7F_1$ and $^5D_0\rightarrow{}^7F_2$ emission bands in the order of 100–200 cm^{-1} caused by the ligand field. The $^7F_0$ state is nondegenerate and, therefore, the $^5D_0\rightarrow{}^7F_0$ emission band does not exhibit ligand field splitting. The single peak at 579 nm in the emission spectrum, therefore, indicates that there is only one luminescent Eu(III) species in solution. With this conclusion, the intensity ratio of the $^5D_0\rightarrow{}^7F_2$ transition and the $^5D_0\rightarrow{}^7F_1$ transition is a good measure of the nature and symmetry of the coordination sphere. In a centrosysmmetric environment, the MD $^5D_0\rightarrow{}^7F_1$ transition of Eu(III) is dominating. Whereas distortion of the symmetry around the ion causes an intensity enhancement of the hypersensitive $^5D_0\rightarrow{}^7F_2$ transition, which means an increased radiative ED probability and consequently a decreased excited state lifetime.

In order to get a further understanding on correlation between ligand coordination sphere and excited state lifetime, A_{MD}, Ω_2 and the calculated $^5D_0\rightarrow{}^7F_2$ emission probability ($A_{^5D_0\rightarrow{}^7F_2}$) as well as experimentally recorded $^5D_0\rightarrow{}^7F_2$ radiative lifetime (τ) are calculated and summarized in Table 2. It is confirmed that the spontaneous MD emission probability of $^5D_0\rightarrow{}^7F_1$ transition is independent of the coordination sphere as we mentioned and localizes in a restrict region of 34.6–34.9 s^{-1}. While, the hypersensitive $^5D_0\rightarrow{}^7F_2$ transition is more sensitive to coordination sphere, this can be seen from the obvious variation of Ω_2. Emission probabilities of $^5D_0\rightarrow{}^7F_1$ transition and $^5D_0\rightarrow{}^7F_2$ transition are the dominating components for total emission probability as shown by emission band intensities in Fig. 3. Compared with A_{MD} and Ω_2 of Eu(DBM)$_3$phen, those of DPDBM-based Eu(III) complexes demonstrate no obvious difference, which means that ligand coordination sphere is not the dominating factor leading to the largely decreased excited state lifetimes. Considering energy transfer mechanism of the Eu(III) complexes as discussed, we come to a conclusion that the decreased excited state lifetimes are caused by the radiative decay suppression of DPDBM which means that there may be energy return from excited Eu(III) ion back to singlet state of DPDBM, offering a novel way leading to shortened excited state lifetime of Eu(III)-based emitter.

Besides, it is found that the excited state lifetime of Eu(DPDBM)$_3$DPPZ is smaller than those of other three Eu(III) complexes. According the previous report, there is potential energy return from excited Eu(III) ion to DPPZ due to DPPZ's low triplet state energy level [13]. Similarly, PL quantum efficiency of Eu(DPDBM)$_3$DPPZ is also the smallest, which can be explained by DPPZ's energy return as well. Although both radiative decay suppression of DPDBM and energy return of DPPZ lead to shortened excited state lifetime, the latter one should be avoided because DPPZ's triplet is nonemissive, and thus leads to energy exhaustion.

4. Conclusion

In this paper, we synthesized four Eu(III) emitters based on a novel triphenylamine-derived beta-diketone ligand. Their excited state lifetimes are dramatically shorter than the usual ones. A detailed analysis reveals that the unique energy transfer mechanism, which means a energy transfer process from singlet state of ligand to $^5D_0$ of Eu(III) ion, is responsible for the largely decreased excited state lifetime. This result provides a practicable method leading to the strongly needed short-lived Eu-based emitters in OLEDs.

Acknowledgements

The authors gratefully thank the financial supports of One Hundred Talents Project from Chinese Academy of Sciences and the National Natural Science Foundations of China (Grant no. 50872130).

Reference

[1] C.W. Tang, S.A. Vanslykc, Appl. Phys. Lett. 51 (1987) 913.
[2] C. Adachi, M.A. Baldo, S.R. Forrest, J. Appl. Phys. 87 (2000) 8049.
[3] X.T. Tao, H. Suzuki, T. Wada, H. Suzuki, S. Miyata, Appl. Phys. Lett. 75 (1999) 1655.
[4] J. Wang, R. Wang, J. Yang, Z. Zheng, M.D. Carducci, T. Cayou, N. Peyghambarian, G.E. Jabbour, J. Am. Chem. Soc. 123 (2001) 6179.
[5] J. Kido, K. Nagai, Y. Okamoto, Chem. Lett. 235 (1991) 1267.
[6] H. Xin, F.Y. Li, M. Guan, C.H. Huang, M. Sun, K.Z. Wang, Y.A. Zhang, L.P. Jin, J. Appl. Phys. 94 (2003) 4729.
[7] C.J. Liang, D. Zhao, Z.R. Hong, D.X. Zhao, X.Y. Liu, W.L. Li, J.B. Peng, J.Q. Yu, C.S. Lee, S.T. Lee, Appl. Phys. Lett. 76 (2000) 67.
[8] M.A. Baldo, C. Adachi, S.R. Forrest, Phys. Rev. B 62 (2000) 10967.
[9] L. Zhang, B. Li, B. Lei, Z. Hong, W. Li, J. Lumin. 128 (2008) 67.
[10] M. Windholz, The Merck Index: An Encyclopedia of Chemicals and Drugs, Merck & Co. Inc., New Jersey, 1988, p. 2991.
[11] B. Lei, B. Li, H. Zhang, L. Zhang, W. Li, J. Phys. Chem. C 111 (2007) 11291.
[12] B. Liang, M.Z. Zhu, W.G. Zhu, Chin. Chem. Lett. 14 (2003) 43.
[13] E.B. van der Tol, H.J. van Ramesdonk, J.W. Verhoeven, F.J. Steemers, E.G. Kerver, W. Verboom, D.N. Reinhoudt, Chem. Eur. J. 4 (1998) 2315.
[14] G.E. Buono-Core, H. Li, Coord. Chem. Rev. 99 (1990) 55.
[15] L. Huang, K.Z. Wang, C.H. Hunag, F.Y. Li, Y.L. Huang, J. Mater. Chem. 11 (2001) 790.
[16] W.T. Carnali, P.R. Fields, K. Rajnak, J. Chem. Phys. 49 (1968) 4244.